

UNDERSTANDING NEURAL NETWORK SYSTEMS FOR IMAGE ANALYSIS USING VECTOR SPACES

Rebecca Pattichis

Dept. of Computer Science
University of California, Los Angeles
Los Angeles CA, USA
pattichi@g.ucla.edu

Marios S. Pattichis

Dept. of Electrical and Computer Engineering
University of New Mexico
Albuquerque NM, USA
pattichi@unm.edu

ABSTRACT

There is strong interest in developing mathematical methods that can be used to understand complex neural networks used in image analysis. In this paper, we introduce techniques from Linear Algebra to model neural network layers as maps between signal spaces. First, we demonstrate how signal spaces can be used to visualize weight spaces and convolutional layer kernels. We also demonstrate how residual vector spaces can be used to further visualize information lost at each layer. Second, we introduce the concept of invertible networks and an algorithm for computing input images that yield specific outputs. We demonstrate our approach on two invertible networks and ResNet18.

1. INTRODUCTION

While neural networks systems perform extremely well in image analysis tasks, there is still a lack of understanding of which image representations are best captured by different layers. With their increasing size and integration into important applications (e.g., biomedical [1]), it is critical for models to become interpretable. The goal of this paper is to suggest methods for understanding neural networks based on the use of vector spaces and Linear Algebra.

Earlier efforts on visualizing neural network layers suggested determining inputs that maximize the activation function for a given input image [2]. In [3], the authors introduced the use of saliency maps that allowed us to verify that specific regions of an image contributed to its classification score. In a recent survey [4], the authors summarize many efforts to interpret neural networks, including the standard practice of visualizing the convolution filters.

Our focus differs from prior approaches by focusing on developing layer interpretations based on the four fundamental vector spaces associated with the weight matrix. We develop signal and residual (rejected signal) spaces to understand how input images get transformed into output images and what image components are removed from each layer. We introduce the concept of invertible neural networks (INNs)

that describe INNs composed of invertible layers where the signal vector spaces can be recovered from the output spaces directly. Similar to [3], we compute input vectors for different network outputs based on a variety of methods. We demonstrate our approach on invertible neural networks and ResNet18, a more complex network.

The rest of the paper is broken into three sections. We describe the methodology in section 2, provide results in section 3, and give concluding remarks in 4.

2. METHODS

We define the four fundamental spaces in section 2.1. We then proceed to provide interpretation of weight vectors using projections in section 2.2. We extend our approach to weight matrices in section 2.3. We then consider computing input image vectors that produce desirable outputs in section 2.4.

2.1. The four fundamental signal spaces

Let x denote the flattened vector input to a neural network layer. Here, x can represent an input image (or video). However, for the purposes of what we are trying to show, we view x as a column vector. We model the output using:

$$\text{Out} = f(Wx + \text{bias}), \quad (1)$$

where W denotes the weight matrix, bias denotes the bias vector, f denotes the activation function, and Out denotes the output vector. In what follows, we consider the zero-bias case. Here, we note that convolutions represent special cases of the weight matrix. Alternatively, for CNN layers, we consider signal spaces on the convolution kernels themselves.

For the purposes of our development, we define y using:

$$y = Wx. \quad (2)$$

We make sense of $y = Wx$ using four fundamental spaces. We define the **signal space** using:

$$\begin{aligned} \text{Signal}(W) &= \text{RowSpace}(W) \\ &= \{x \in \mathbf{R}^n \mid x = W^T v \text{ for some } v \in \mathbf{R}^m\}. \end{aligned}$$

The signal space represents what W interprets as the signal component of x . After processing the signal, we are led to study the column space, redefined here as the **signal output space** Wx given by:

$$\begin{aligned} \mathbf{SignalOut}(W) &= \mathbf{ColumnSpace}(W) \\ &= \{y \in \mathbf{R}^m \mid y = Wx \text{ for some } x \in \mathbf{R}^n\}. \end{aligned}$$

The **signal output space** represents the set of output images that we can reach for any given input image.

We now have the elegant equation that maps the signal images $x_{\text{signal}} \in \mathbf{Signal}(W)$ to the reachable output images $y_{\text{signal-out}} \in \mathbf{SignalOut}(W)$:

$$Wx_{\text{signal}} = y_{\text{signal-out}}. \quad (3)$$

We note that the pseudoinverse W^+ solves equation (3) exactly using $x_{\text{signal}} = W^+y_{\text{signal-out}}$.

In contrast to the signal space, we define the **rejected signal space** in terms of the null-space of W :

$$\begin{aligned} \mathbf{RejSignal}(W) &= \mathbf{NullSpace}(W) \\ &= \{x \in \mathbf{R}^n \mid Wx = 0\}. \end{aligned}$$

Here, we note that the rejected signal space describes all of the input images that have no impact on the outputs! Similarly, in contrast to the output space, we define the **rejected output space** using the left null space of W :

$$\begin{aligned} \mathbf{RejSignalOut}(W) &= \mathbf{LeftNullSpace}(W) \\ &= \{y \in \mathbf{R}^m \mid W^T y = 0\}. \end{aligned}$$

The input image space is decomposed into the signal and rejected signal spaces as given by [5]

$$\begin{aligned} \mathbf{R}^n &= \mathbf{ColumnSpace}(W^T) \oplus \mathbf{NullSpace}(W) \\ &= \mathbf{Signal}(W) \oplus \mathbf{RejSignal}(W). \end{aligned}$$

The output image space is decomposed into the signal output space and the rejected signal output space as given by:

$$\begin{aligned} \mathbf{R}^m &= \mathbf{ColumnSpace}(W) \oplus \mathbf{NullSpace}(W^T) \\ &= \mathbf{SignalOut}(W) \oplus \mathbf{RejSignalOut}(W). \end{aligned}$$

2.2. Understanding weight vectors using projections

Let w denote the weight column vector associated with a single neuron. In this case, $w^T x$ lies in the $\mathbf{Signal}(W = w^T)$ space. Here, the projection of x onto w is a scaled version of $w^T x$ given by:

$$p = \left((w^T x) / \|w\|^2 \right) x, \quad \|w\|^2 = w^T w.$$

In this case, the weight vector completely removes the signal components that belong to $\mathbf{RejSignal}(W = w^T)$ given by:

$$\text{residual} = x - p \quad \text{satisfying} \quad (x - p)^T w = 0, \quad (4)$$

where residual refers to the residual image component that is ignored by the weight vector! In terms of explainability, we want to examine the residual image to make sure that it does not contain any important signal components. It is also interesting to note that the input image energy is distributed between the projection on $\mathbf{Signal}(W = w^T)$ and $\mathbf{RejSignal}(W = w^T)$ spaces as given by: $\|x\|^2 = \|p\|^2 + \|\text{residual}\|^2$. Thus, we can also measure the amount of image energy removed by the residual using: $\|\text{residual}\|^2 / \|x\|^2$.

2.3. Understanding weight matrices using signal spaces

We compute the signal spaces using the Singular Value Decomposition: $W = U\Sigma V^T$. Along the diagonal of Σ , we have the associated singular values: $\sigma_1 \geq \sigma_2 \geq \dots \geq \sigma_r \geq 0$, where r denotes the rank of the matrix and σ_1/σ_r denotes the condition number of W . Here, we note that a low condition number (near 1) is required for stable decompositions. A high condition number would indicate instability in the signal space decomposition.

The four fundamental spaces are built using the eigenvector decompositions of the symmetric matrices WW^T and $W^T W$. We map inputs in $\mathbf{Signal}(W)$ to $\mathbf{SignalOut}(W)$ using the unit eigenvectors of each space as given by:

$$\sigma_1 v_1, \dots, \sigma_r v_r, \quad (5)$$

where we can visualize the relative importance of each eigenvector through its corresponding singular vector. More generally, we have:

$$x = x_{\mathbf{Signal}(W)} + x_{\mathbf{RejSignal}(W)},$$

where the components are given using:

$$\begin{aligned} x_{\mathbf{Signal}(W)} &= a_1 v_1 + a_2 v_2 + \dots + a_r v_r \\ x_{\mathbf{RejSignal}(W)} &= a_{r+1} v_{r+1} + \dots + a_n v_n \end{aligned}$$

and $a_i = v_i^T x$ gives the coefficients.

2.3.1. Simplified interpretation of convolutional layers

We consider a simplified interpretation of convolutional layers using the convolution kernels. Here, we replace the rows of W with the flattened convolutional kernels. Hence, our signal spaces refer to the mapping between the support of each kernel and the output pixels.

2.4. Input image generation based on ideal outputs and invertible networks

We consider the problem of computing inverse maps given desirable outputs. Here, we note that vector spaces offer a solution provided that we use activation functions that are fully

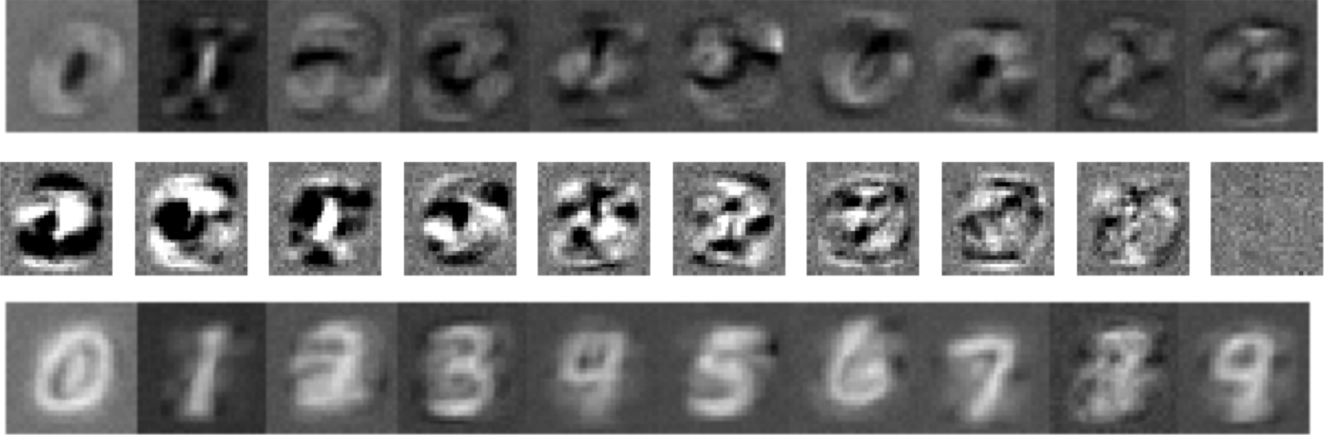


Fig. 1: Vector spaces for a single-layer fully connected neural network applied to the MNIST digits dataset. The top row represents the original weights. The middle row represents the signal space: $\sigma_0 v_0, \dots, \sigma_9 v_9$. The condition number is 7.22. The last row represents the residual vectors when the network is applied to the average of each digit class (see equation (4)).

invertible (e.g., SELU, $\tanh(\cdot)$, sigmoid). In this case, we can iteratively invert each layer to recover the signal components using:

$$x_{\text{Signal}(W)} = W^+ f^{-1}(\text{Out} - \text{bias}). \quad (6)$$

Unfortunately, for non-invertible activation functions, we will need to redefine the vector spaces using convex polytopes. More generally, we consider a computational approach that is generally applicable to any neural network. Here, we seek to find the input image that generates the minimum distance from an ideal output. To obtain realistic images, we use the maxima and minima values achieved over the training set to define the ideal output vectors. For example, the ideal output for the first category would have the max value over the first output and the minimum value over the rest of them.

We consider two approaches for estimating input images for ideal outputs. First, we try to minimize the distance to the ideal outputs over the training set. We define the *avg-img* to be the average image over all of the training images for the training class that we are interested in. We define the *min-img* to be the training image that minimizes the distance over the set of all training images. We generalize the *min-img* using the *avg-min-img* that is defined to be the average image over the training images that are within the lowest 25th percentile of distances to the ideal output. Similar to [3], we also train the input layer with frozen weights to see if we can produce an input image that is even closer to the ideal output.

3. RESULTS

We demonstrate our approach on three neural network architectures using the standard MNIST 10-class classification problem. First, we consider two fully connected neural networks (FCNN): (i) a 1-layer FCNN, and (ii) a 5-layer FCNN

with output dimensions of 256, 256, 128, 32, and 10. We used SELU activation functions so that they were invertible as discussed in section 2.4. Second, we consider the ResNet18 as an example of a more complex neural network architecture. We trained all three networks using a learning rate of 0.001, momentum=0.9 and 20 epochs. In order of neural network complexity, we got high classification accuracies at: (i) 92% for 1-layer FCNN, (ii) 97% for 5-layer FCNN, and (iii) 99% for ResNet18. In what follows, we provide interpretations for different layers of the architectures.

We show three vector spaces for the 1-layer FCNN in Fig. 1. From the signal space, we can clearly see the decreasing importance of the signal vectors. For example, $\sigma_9 v_9$ represents mostly noise, and it is far less bright than $\sigma_0 v_0$ ($\sigma_0/\sigma_9 = 7.22$). On the other hand, unlike the weight vectors of the top row, the rest of the signal vectors (middle row) exhibit strong binarized components, dominated by bright and dark regions. The last row of images shows the residual images for the average digit from each class. Here, it is interesting to note the effectiveness of the weights for 8. For 8, the residual image is unrecognizable, as expected. For 0, the residual fills in the middle hole, implying that this represents a strong deviation from the average 0 image. The rest of the residual images show strong signal components that are likely due to the lack of translational invariance of the network when applied to average vectors (e.g., see residual for 1).

We present the signal space for the first convolutional layer of ResNet18 in the first Sequential layer in Fig. 2. Here, we note that this layer consists of $64 \times 64 = 4096$ 3×3 kernels that we represent with just 9 signal vectors $\sigma_1 v_1, \dots, \sigma_9 v_9$. We note the strong directional selectivity of the signal kernels. Similar to the binarized patterns of the middle row of Fig. 1, we find pixel dominance in different locations or directions. For example, we have left vertical



Fig. 2: The signal space for the first 2D convolution layer in the first Sequential layer of ResNet fine-tuned for MNIST classification (99% accuracy, 1.07 condition number).

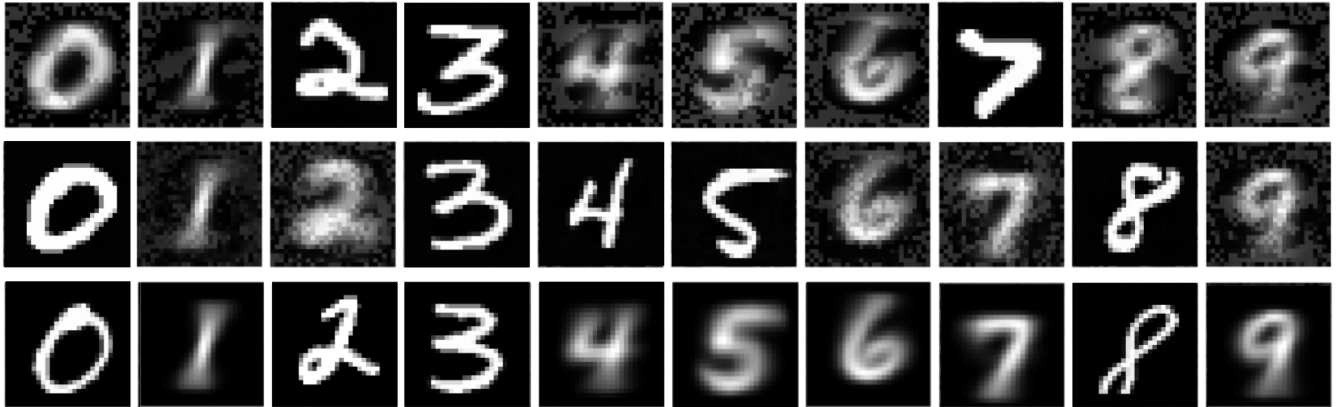


Fig. 3: Generated ideal input images for each digit using different algorithms (see section 2.4). Top row: 1-layer FCNN (92% accuracy): *avg-img+training* for 0, 1, 4, 5, 6, 8, and 9; *min-img+training* for 2, 3, and 7. Middle row: 5-layer FCNN (97% accuracy): *avg-img+training* for 1, 2, 6, and 7; *min-img+training* for 0, 3, 4, 5, 8, and 9. Bottom row: ResNet128 (99% accuracy): *avg-img* for 1, 4, 5, 6, 7, and 9; *min-img* for 0, 2, 3, and 8 that look binarized; *avg-min-img* for 4.

column dominance in $\sigma_1 v_1$, single pixel (lower-center) dominance in $\sigma_2 v_2$, top and bottom row dominance in $\sigma_7 v_7$, and lower-left diagonal dominance in $\sigma_9 v_9$. Furthermore, since the condition number is 1.07, it is clear that the signal kernels are of equal importance.

We generate input images for each network and each category in Fig. 3. For ResNet, we note that training did not improve the images that were generated by *avg-img*, *min-img*, *avg-min-img*. This explains why the ResNet images appear either binarized (*min-img*) or blurry (for *avg-img*, *avg-min-img*). On the other hand, our low-complexity networks proved much easier to train. Either way, it is clear that our approach of initializing based on the original training images proved very effective.

4. CONCLUSION

The paper introduced the use of the four fundamental vector spaces to understand how weight spaces and residual spaces map input images to output images. Weight spaces represent image (signal) content that gets mapped to the output images. Residual spaces represent the rejected image content that does not propagate through the network. The paper also discussed invertible networks and discussed methods that estimate input images that yield specific outputs. In future research, it

will be interesting to explore if invertible networks can match the performance of non-invertible networks. We note that invertible networks allow us to easily backproject output vector spaces to input image spaces.

5. REFERENCES

- [1] N. Prentzas, A. Kakas, and C. S. Pattichis, “Explainable AI applications in the medical domain: A systematic review,” 2023. [Online]. Available: <https://arxiv.org/abs/2308.05411>
- [2] D. Erhan, Y. Bengio, A. Courville, and P. Vincent, “Visualizing higher-layer features of a deep network,” *Technical Report, Univeristé de Montréal*, 01 2009.
- [3] K. Simonyan, A. Vedaldi, and A. Zisserman, “Deep inside convolutional networks: Visualising image classification models and saliency maps,” 2014.
- [4] A. Shahroudjed, “A survey on understanding, visualizations, and explanation of deep neural networks,” *CoRR*, vol. abs/2102.01792, 2021. [Online]. Available: <https://arxiv.org/abs/2102.01792>
- [5] G. Strang, *Introduction to linear algebra*. SIAM, 2022.